國立交通大學
光電工程學系　光電工程研究所
碩士論文

偏壓對有機薄膜電晶體氣體感測器之影響以及相關機制

Influence of bias on OTFT gas sensor and its sensing mechanism

研究生：梁芸嘉
指導教授：冉曉雯　博士

中華民國 九十六年 七 月

偏壓對有機薄膜電晶體氣體感測器之影響以及相關機制

Influence of bias on OTFT gas sensor and its sensing mechanism

研 究 生：梁芸嘉　　Student：Yun-Chia Liang

指導教授：冉曉雯 博士　　Advisor：Dr. Hsiao-Wen Zan

國 立 交 通 大 學

光電工程學系　光電工程研究所

碩 士 論 文

A Thesis

Submitted to Department of Photonics & Institute of Electro-Optical Engineering

College of Electrical Engineering and Computer Science

National Chiao Tung University

in partial Fulfillment of the Requirements

for the Degree of

Master

in

Electro-Optical Engineering

June 2007

Hsinchu, Taiwan, Republic of China

中 華 民 國 九 十 六 年 七 月

偏壓對有機薄膜電晶體氣體感測器之影響以及相關機制

研究生:梁芸嘉　　指導教授:冉曉雯 博士

國立交通大學

光電工程研究所碩士班

摘要

近年來有機薄膜電晶體氣體感應器已經引起大量的研究,此成果之應用範圍包含食物品質檢測以及醫療用自我檢測儀器。為了達成能商業量產的價值,我們需要製造出成本低廉且高度靈敏的感測元件,為了達成這個目的,我們選用有機電子材料來製造氣體感測器。

現有的相關研究多著重在氣體感測器電流值的變化,對於其他參數如臨界電壓以及載子移動率卻缺乏討論。我們希望站在元件物理的基礎上更深入的探討氣體反應的相關機制。

在氣體感應的量測中我們觀察到造成電流值變化的主因是因為臨界電壓的漂移。隨著氨濃度的增加,臨界電壓值的移動也會更劇烈,但當氨氣移除之後臨界電壓有恢復到初始狀態的趨勢。故我們認為氨氣與五苯環分子的作用為一種吸附現象。在這實驗中我們發現一個很有趣的現象:當三顆特性相同的有機元件放

在同一個有氨的環境中，不論放置在這環境中多長時間所量測到的初始臨界電壓都相近，這結果暗示我們氣體感測的行為與閘極偏壓有關。

在長時施加閘極偏壓的氣體感測中，固定施加的偏壓改變氣體濃度，當氨氣濃度越高臨界電壓變動也增加。若固定氣體濃度施加更高偏壓也會看到相同的情形。不論是在有無偏壓實驗條件下，氣體擴散模型可以成功解釋氨在五苯環薄膜中的擴散行為。

Influence of bias on OTFT gas sensor and its sensing mechanism

Student: Yun-Chia Liang Advisor: Dr. Hsiao-Wen Zan

Institute of Electro-Optical Engineering

National Chiao Tung University

Abstract

Electronic noses have attracted lots of interests in the recent years. It can be used from food-quality monitoring to medical self-diagnosis kits. For commercial purpose, we need to produce low-cost and high sensitivity electronic noses. To reach these targets, we used organic material to fabricate electronic nose.

Most of the previous works focused on the electric current effect alone. In this work we also studied the effect on threshold voltage 、 mobility, from which we investigated the mechanism for gas sensing.

In this experiment, we observed that the electric current variation was strongly influenced by the threshold voltage. When the ammonia concentration was increased, the threshold voltage became larger. But we noted that the threshold voltage tend to recover when the ammonia was removed. For this reason, we consider that the

reaction between ammonia and pentacene is basically an absorption reaction. At the same time, we observed an interesting phenomenon: we measured three identical devices that were placed at the same distance from the gas source. When the measurement was applied on the three devices one after another along with the NH_3 sensing time, we observed an interesting event- these three devices had similar initial threshold voltages no matter how long these devices had been exposed to the NH_3 gas. This result implied that the sensing behavior may have a strong correlation with the gate bias.

In the experiment of bias stress gas sensing, we applied a fixed gate bias and varied the ammonia concentration. The threshold voltage became larger with the ammonia concentration was increased. We observed the same result when we applied higher gate bias and added a fixed amount of ammonia. Our results showed that Fick's second law can successfully explain the variations of threshold voltage.

Acknowledgment

首先誠摯的感謝指導教授冉曉雯博士，老師不論在實驗上或者生活上都給予我很好的建議以及鼓勵，這兩年在老師身上學到很多使我個人也成長不少，在此獻上最誠摯的謝意。

本論文的完成亦得感謝博士班學長國錫、士欽以及政偉，在實驗上給予很多的指導以及照顧。尤其士欽學長在我實驗量測上給予相當多的幫助，讓我得以順利完成實驗。也很高興能與文馨、而康、光明、德倫、廷遠、皇維、睿志一起度過這難忘的兩年，感謝你們在實驗上以及各方面的協助。

兩年的生活有苦有樂，謝謝多媒體工程所的詠恬、網路工程所的雅琳、以及資工所的慧伶陪我一起度過。謝謝你們這一路的關懷以及陪伴，幫助我度過許多艱辛的時刻。希望不論是出國還是留在國內念博士的你們都會相當順利。

最後，感謝父母給我最大的空間讓我做自己想做的事。無悔的栽培讓我順利完成碩士學位。謝謝你們這 24 年來的照顧，謝謝。

Contents

Figure Captions

Chapter 1

Chapter 2

Chapter 3

Chapter 1

Introduction

1-1. Introduction of organic thin film transistor (OTFT)

The conductance of organic molecules was discovered in 1940s [1]. It began from a very small number of preliminary works on conjugated small molecules [2,3] and polymers[4]. The first transistor based on an organic semiconductor was only reported in 1986 with a device made on an electrochemically grown polythiophene film [5]. Polythiophene belongs to the family of the conducting polymers that were discovered in the late 1970s [6]. The inventors of polyacetylene were awarded the Nobel Prize in chemistry in 2000. The possibility of fabricating organic thin-film transistors (OTFTs) with small conjugated molecules was demonstrated in 1989 with sexithiophene, an oligomer of polythiophene made of sixthiophene rings linked at alpha position [7]. For a decade, there have been a lot of researches about better-performing organic thin-film transistors (OTFTs). Now the performances of OTFTs are comparable to the hydrogenated amorphous silicon TFTs (a-Si:H TFT) [8]. OTFTs have many advantages compared to other electronic devices. The low production cost and the low fabrication temperature enable OTFTs to be used on large-area electronic applications including flexible displays, smart cards, radio

frequency identification cards (RFIDs), sensors and electronic paper. For these reasons, more and more industrial groups have recently initiated research programs in the field of organic transistors. Until recently, much of the research effort has been directed at improving the charge-carrier mobility. Several papers have reviewed this search for better materials and device architecture [9-13].

1-1.1 Organic materials

A number of organic materials such as polythiophene, α- sexithiophene (α-6T) have been investigated for use in field effect transistors (FETs) [14]. Polycrystalline molecular solids such as α-sexithiophene (α-6T) or amorphous/semi-crystalline polymers such as polythiophene or acenes such as pentacene, teracene show the highest mobilities [15]. Dimitrakopoulos *et al* [16] shows the evolution of organic materials and the improvement in their mobilities over the years. Pentacene based FETs exhibit high mobilities and have been extensively studied. Pentacene is made up of five benzene rings as shown in Fig. 1-1. It has a sublimation temperature of 300℃. Well ordered pentacene films can be deposited at low temperatures, this makes it suitable for applications on plastic substrates.

1-1.2 OTFT device structure

In organic thin film transistor, the organic film can be deposited by evaporation, spin-on or ink-jet printing. And the devices can be fabricated on a number of substrates like silicon, glass and plastic. Figure 1-2(a) and (b) illustrate a widely used structure of OTFTs: top-contact structure (Fig.1-2(a)) and bottom-contact structure (Fig.1-2(b)).

In top-contact structure, a heavily doped silicon substrate acts as a gate electrode for the device. Thermally grown silicon dioxide is deposited on the substrate as gate insulator. Next, the organic material is deposited on the insulator and the metal is deposited on the top of the organic semiconductor as the source and the drain electrodes. Because the organic layer is sensitive to the photolithographic patterning and chemical etching. The source and drain electrodes are defined through the shadow mask.

The other popular structure is the bottom-contact structure, in which the organic layer is deposited directly on the top of the structure. The structure is commonly used in the field of organic electronics due to the easy fabrication. The entire structure except for the organic layer can be patterned using photolithography technology. However, they usually have inferior device performances than the ones with

top-contact structure. The difficulty to obtain well-ordered organic film on metal electrodes may be the primary reason.

1-1.3 Operating mechanisms of organic thin film transistor

The gate structure of thin-film transistors operates like a capacitor. When a voltage is applied between source and gate, a charge is induced at the insulator-semiconductor interface. This charge forms a conducting channel, the conductance of which is proportional to the gate voltage. At low drain voltages, the current increases linearly with drain voltage, following the Ohm's law. When the drain voltage is compared to gate voltage, the voltage drop at drain contact falls to zero and the conducting channel is pinched off. This corresponds to the so-called saturation regime where the current becomes independent of the drain voltage. In the transfer characteristic, the current is plotted as a function of the gate voltage at a constant drain bias. Below a given threshold, the current increases exponentially. This corresponds to the below-threshold regime. In the above threshold regime, the current becomes proportional to the gate bias, as expected from the above description of the operating mode of the transistor.

The Fermi level of gold and the band diagram of pentacene are shown in Fig. 1-3. When a positive voltage is applied to the gate, negative charges are induced at the

source electrode. As can be seen in Fig. 1-3, the Fermi level of gold is far away from the LUMO level, so that electron injection is very unlikely. Accordingly, no current passes through the pentacene layer, and the small measured current essentially comes from leaks through the insulating layer. When the gate voltage is reversed, holes can be injected from the source to the semiconductor, because the Fermi level of gold is close to the HOMO level of pentacene. Accordingly, a conducting channel forms at the insulator-semiconductor interface. The charges can be driven from the source to the drain by applying a drain bias. For this reason, pentacene is said to be a *p*-type semiconductor. However, it should be pointed out that this concept differs from that of doping in conventional semiconductors, which can be made either *n*-type or *p*-type by introducing a large amount of an electron donating or electron withdrawing element. Symmetrically, an organic semiconductor will be said *n*-type when the source and drain electrodes can inject electrons in its LUMO level, provided electron transport does occur, i.e., electron mobility is not too low.

1-2. Ammonia sensors and their applications [7]

1-2.1 Application areas of ammonia sensors

Ammonia is an obvious gas in the world. Apart from its natural origin, there are many sources of ammonia, such as the chemical industry or intensive life-stock. Subsequently, different application areas for gaseous ammonia sensors are investigated, such as:

(1) Automotive industry

The application for ammonia sensors in the automotive area is NO_x reduction in diesel engines. Because modern diesel engines cause large concentrations of NO or NO_2 [8.9], people use selective catalytic reduction (SCR) of NO_x with NH_3 to reduce the toxic NO_x concentrations. The formula is shown in equation (1-1) [10].

$$4NO + 4NH_3 + O_2 \rightarrow 4N_2 + 6H_2O \quad (1\text{-}1)$$

But adding too much ammonia causes the other pollution, known as ammonia-slip. Therefore, measuring the excess ammonia concentration in the exhaust system is also important.

(2) Chemical industry

The chemical industry, fertilizer factories and refrigeration systems use almost pure ammonia. If there is a leak in the facility, high concentrations of ammonia form a threat to the human health. Therefore these facilities should have an alarm system detecting and warning for dangerous ammonia concentrations.

(3) Medical applications for ammonia sensors

By measuring ammonia level in exhaled air, the ammonia sensor can be a fast diagnostic method for patients with disturbed urea balance, like kidney disorder [11] or ulcers. These diseases are caused by *H.pylori* bacterial stomach infection. Now, the common way to detect the *H.pylori* bacterial is an endoscopic procedure. But the endoscopic procedure is an invasive and inconvenient test. In order to develop the more convenient way to detect the *H.pylori* bacterial, the non-invasive test methods based on measuring exhaled CO_2 or NH_3 level was mentioned [12,13].

1-2.2 Different types of ammonia sensor

(1) Metal- oxide gas sensors

A lot of research about metal-oxide gas sensor have been done [14], especially in Japan [15]. These sensors are rugged and inexpensive and thus very promising for the developing gas sensors. In this kind of gas sensor, WO_3 based sensing material is used to respond to ammonia [16,17]. But it must be operated at the elevated temperature of more than 400℃ [17].

(2) Catalytic ammonia sensors

By a change in ammonia concentration, the charge carrier concentration in the catalytic metal is altered. The selectivity of these sensors depends on these parameters, such as the catalytic metal, the morphology of the metal layer and the operating

temperature. But for this kind of gas sensor, the lower detection limit is normally in the low-ppm range and the accuracy is limited.

(3) Optical gas analyzers

There are two main optical ammonia analyzers. One is based on a change in color as ammonia reacts with a reagent. The other is optical absorption detection applied as a method to sense ammonia. But the equipments for the optical gas analyzer are large and expensive.

(4) Conducting polymer gas detectors

The polymer is supposed to be deprotonated by ammonia and the conduction of the polymer is also changed [18]. Comparing with other types of ammonia gas sensor, there are some advantages of conducting polymer gas detectors, like lower detection limit (0.5 ppm)、faster response time (60s-100s) and it can be operated at room temperature. In the beginning, gas sensors are chemoresistor sensors. But using a three- terminal TFT structure instead of two-terminal chemoresistor construction is based on gate bias can enhance sensitivity, discrimination and repeatability [19-23]. Furthermore the transistor can offer multi-parameters for different analytes, such as bulk conductivity、 threshold voltage、 field effect mobility and field- induced conductivity [19].

1-3. OTFT gas (ammonia) sensor

Many experiments have demonstrated the sensing ability of OTFT by using different organic materials and different gaseous analytes [19.24]. The reasons for organic thin film transistor can be good gas sensors are as follow. First, OTFTs have some advantages, such as simple process、low fabrication costs and for large area. Second, the organic materials are made up by the carbon backbones. The carbon backbones make the organic devices have higher chemical activity than other inorganic devices. Moreover, by synthetic chemistry we can deposit specific active layer to control and adjust the sensitivities and selectivity of gas sensors [25].

Due to the chemical activity of the carbon backbone, the conducting polymers can sense a wide range of analytes, including humidity, nitrogen and other organic compounds.

For OTFT gas sensors, the morphology of the active layer and the molecular structure of both semiconductor and gas molecule are all important factors for the gas response. An associated research by Torsi *et al* [26], it has been reported that the result of various oligothiophene films to exposure alcohol. The response is highly dependent on the amount of grain boundaries. But for other gas species like octanenitrile, no grain boundary effect has been observed. These results show that the interaction mechanisms are different depending on the nature of semiconductor and

analyte species. For this reason, Torsi et al. have proposed multi-parameter OTFT gas sensors [19]. OTFT exhibit many sensing index such as the on-state conductivity, the threshold voltage, the mobility, the off-state conductivity and the subthrehsold swing, etc. These parameters can be used as “fingerprints” to response the OTFT for a given chemical compound.

Recently, nanoscale organic thin film transistors were fabricated as gas sensors. The sensing behavior of these small dimension devices is markedly different from that of larger devices for the same analyte [27].

1-4. Motivation

In the previous study, OTFTs can respond with ammonia was mentioned. In order to control the NH_3-gas sensor, studying the sensing mechanism in depth is necessary. On the other hand, some groups observed that gate bias can enhance the sensitivity. Therefore, in our experiment, the gas sensing behaviors with and without were discussed

1-5. Thesis organization

In Chapter 1, we briefly introduce the OTFTs and the current ammonia sensors. In Chapter 2, the device fabrication procedure, measurement environment, experiment design and parameter extraction of OTFTs are presented. In Chapter 3, the NH_3-sensing phenomena with and without bias stress are investigated. The gas diffusion model- Fick's second law is used to explain the gas sensing phenomena. Finally, the conclusion is given in Chapter 4.

Chapter 2

Experiments

2-1. The Fabrication for OTFTs

Conventional bottom-gate top-contact OTFTs were used in this experiment. The structure is shown in Fig.2-1.

The detail fabrication processes are as follows:

Step1. Substrate and gate electrode

Heavily-doped single crystal silicon wafer was used as substrate and gate electrode.

Step2. Gate oxide formation

After RCA cleaning, the 1000Å thermally grown SiO_2 layer was deposited in furnace.

Step3. Pentacene film deposition through shadow mask

The pentacene material obtained from Aldrich without any purification was directly placed in the thermal coater for the deposition. It is well known that the deposition pressure, deposition rate, and deposition temperature are the three critical parameters to the quality of the organic film [28]. The deposition is started at the pressure around 3×10^{-6}torr. Slower deposition rate is expected to result in smoother

and better ordering of the organic molecules. The deposition temperature is also a factor influencing the pentacene film formation. The 100-nm-thick pentacene was deposited by thermal evaporation at a deposition rate of 0.5Å/s. During the deposition process, the substrates temperature fixed at 70°C. The active region and source/deain electrodes were all defined by shadow mask.

Step4. Source/Drain deposition through the shadow mask

In order to form the Ohmic contact, pentacene and source/drain electrodes must have similar work function [29]. The work function of gold is about 5.1eV and it can provide a better injection. Gold was deposited 100nm on pentacene film as the source/drain electrodes by using thermal coater. The source/drain region was defined through shadow mask.

2-2. Measurement environment

The gas sensing characteristics were studied according to the method proposed by A.Alec Talin *et al.* [30]. We used a small cotton mass to absorb different amount of pure NH_3, then placed the cotton mass one centimeter from the devices. Because the NH_3 liquid can soon evaporate, the NH_3 gas can react with the OTFT. Then the device characteristics were measured by HP 4156C.

2-3. Experiment Design

The experiment was discussed in two parts: (A) The phenomenon of gas sensing. (B) The bias stress gas sensing.

In part A, in the beginning, the sensing and recovery behavior of NH_3- OTFT sensors were investigated. Then, the threshold voltage variations with different ammonia concentrations were observed. Diffusion model- Fick's second law is used to explain the sensing mechanism. Finally, three identical devices were put in the ammonia environment at the same time and we observed the threshold voltage variations.

In part B, the gas sensing with gate bias was discussed. At first, we applied a constant gate bias and observed the threshold voltage shifts with different concentration. Next, we changed the gate bias stress and investigated the threshold voltage variations in a fixed ammonia concentration.

2-4. Parameter Extraction

In this section, we mention about how to extract mobility (μ), the threshold voltage (V_{th}) and the subthreshod swing (s.s). These parameters can be used to monitor the variation of OTFT gas sensor [19].

2-4.1 Mobility

Mobility (μ) is an important parameter in most electronic devices because it is directly related to the performance of a transistor. It is normalized for channel width, channel length, and dielectric capacitance.

Generally, mobility can be extracted from the transconductance maximum g_m in the linear region:

$$g_m = \left[\frac{\partial I_D}{\partial V_G}\right]_{V_D=constant} = \frac{WC_{OX}}{L}\mu V_D \tag{2.1}$$

$$\mu = \frac{g_m}{(\frac{w}{L}C_{ox}V_D)} \tag{2.2}$$

2-4.2 Threshold voltage

In inorganic electric devices, threshold voltage (V_{th}) is defined as the point at which the channel has been completely inverted. That means when the concentration of inversion charge in the channel equals the equilibrium majority charge carrier concentration in the bulk. But the most commonly used definition for threshold voltage (V_{th}) of an OTFT is extracted from equation (2.3), by extrapolating the linear I_D-V_G plot at I_D=0

$$I_D = \frac{W\mu C_{ox}}{L}[(V_G - V_T)V_D - \frac{V_D^2}{2}] \tag{2.3}$$

In organic semiconductor, the V_{th} is determined primarily by the relative work-function of the gate, source/drain contacts and the organic layer, as well as the fixed charge and trap distributions in the organic layer. Because of run-to-run variations, the parameters can be difficult to suppress. Thus, V_{th} control is an important hurdle to commercialization of OTFTs.

2-4.3 Subthreshod swing

Subthreshold swing is also important characteristics for device application. It is a measure of how rapidly the device switches from the off state to the on state in the region of exponential current increase. Moreover, the subthreshold swing also represents the interface quality and the defect density. Good performance TFTs mean lower subthreshold swing of transistors.

$$S = \frac{\partial V_G}{\partial(\log I_D)}\bigg|_{V_D=\text{constant}} \quad \text{, when } V_G<V_T \text{ for p-type.} \tag{2.4}$$

Chapter 3

Result & Discussion

In this chapter, we investigated the gas sensing mechanism with and without bias stress. In the following experiments, drain voltage is fixed at -6V and gate voltages are changed from 20V to -40V.

3-1 The sensing phenomenon under no bias stress

3-1.1 The electrical properties of OTFT gas sensor

The reactions between OTFTs and the ammonia gas are illustrated in Fig.3-1, 3-2. After we added 2μℓ ammonia into a cotton, we observed the drain current and the transconductance (G_M) were decreased. Then, the mobility (μ) 、the threshold voltage (V_{th}) and the subthreshold swing (S.S) were extracted. The variations of the mobility (μ)、the threshold voltage (V_{th}) and the subthreshold swing (S.S) along with the time in the ammonia environment were depicted in Fig. 3-2. The field-effect mobility and the subthrehsold swing kept almost unchanged, while the threshold voltage exhibited strong dependence on the sensing time. From the above, we supposed the drain current decreases resulted from the variations of mobility and threshold voltage. However the changes of threshold voltage are larger than mobility. We believed the threshold voltage shifts play an important role for current decrease.

In this thesis, we will discuss the gas sensing mechanism through the threshold voltage variations in Fig.3-3.

3-1.2 The recovery phenomenon

In addition to the reactions between OTFTs and ammonia, we looked forward to observing the phenomenon when ammonia gas was removed. We noted the threshold voltage tended to recover after taking away the cotton with ammonia. The phenomenon is shown in Fig. 3-4. At room temperature, the threshold voltage recovery behavior implied that the reaction between ammonia and pentacene is physical absorption, not chemical reactions. We consider that the variation of threshold voltage results from the absorption of ammonia molecules absorbed onto the pentacene surface into the pentacene film through diffusion.

3-1.3 Gas diffusion model

Oana *et al.* [31] used Fick's second law to model the one dimension diffusion of gases into pentacene single crystals. The total quantity of gas molecules in pentacene crystal is obtained by integrating Fick's second law over the length of the diffusion profile. The result is normalized and expressed in molar fraction of gas molecules in

pentacene. An extra term needs to be added in the solution (N_{start}). This term reflects the fact that the measurement starts at t=0 with a quantity of gas that was accumulated in crystal. The equation of modeling the diffusion of gases in pentacene is thus:

$$N(t)=N_{start}+N_{source}\{d[1-erf(\frac{d}{2\sqrt{Dt}})]+\frac{2}{\sqrt{\pi}}\cdot\sqrt{Dt}\cdot[1-\exp(-\frac{d^2}{4Dt})]\} \quad (3\text{-}1)$$

where N(t) is the molar fraction of gas at time t, N_{source} is the gas flow expressed as molar fraction, d is the length of the crystal in the direction in which the one dimension diffusion occurs, and D is the diffusion coefficient. Their result showed the diffusion length is similar to the pentacene film thickness.

We rewrite the equation (3-1) to another form:

$$\frac{N(t)-N_{start}}{N_{source}}=\frac{\Delta N(t)}{N_{source}}=\{d[1-erf(\frac{d}{2\sqrt{Dt}})]+\frac{2}{\sqrt{\pi}}\cdot\sqrt{Dt}\cdot[1-\exp(-\frac{d^2}{4Dt})]\} \quad (3\text{-}2)$$

$\Delta N(t)$ represents the variation of gas in pentacene film in time = t and is expressed as molar fraction. We tried to simulate the relations between equation (3-2) and diffusion coefficient (D)、diffusion length (d) by Matlab . In Fig.3-5, we set diffusion length d as 1000 Å and varied the value of diffusion coefficient D. As the diffusion coefficient became larger, the gases diffuse into the pentacene film faster.

In other words, the response became faster. In Fig.3-6, we fixed the diffusion coefficient D as 10^{-12} cm^2/s and changed the diffusion length d. When the diffusion length increased, the amount of gas that diffused into the pentacene film became larger. From these results, we found if that the value of D/d was larger, the responses of equation (3-2) became faster.

3-1.4 Gas concentration effect

The above all discussion about the gas sensing phenomenon was with a fixed amount of ammonia concentration. In Fig.3-7, we added different amount of ammonia and observed the threshold voltage shifts. When the amount of ammonia increased, the threshold voltage shift also increased. To study the gas sensing mechanism in different ammonia concentration, we used the Fick's second law to fit the experiment results in Fig.3-8. An agreement can be found when the following relationship is proposed.

$$C_{ox}\Delta V_{th} = K\frac{\Delta N(t)}{N_{source}} \tag{3-3}$$

In this relationship, we assumed that the threshold voltage shift was due to the extra charge that came from the gas molecules.K is the ratio of molecules which form the effective charge.

In Fig.3-8, we set diffusion length d as 10^{-5}cm and varied the fitting parameter D、K to obtain the simulation result. In the condition with 2μℓ ammonia, D is $1.5*10^{-13}$ cm^2/s and K is $4.93*10^{-13}$. But in 10μℓ ammonia condition, the fitting parameters are D= $5*10^{-13}$ cm^2/s and K=$5.31*10^{-13}$. The increase of ammonia concentration increased the diffusion coefficient "D" and enhanced the percentage of ammonia molecules which can induce the threshold voltage shift.

3-1.5 The phenomenon of different NH_3 exposed time

In previous experiments, Fick's second law can successfully explain that the ammonia enhanced the threshold voltage shift. But we observed another interesting phenomenon in the ammonia-OTFT sensor.

We measured three identical devices that were placed at the same distance from the cotton mass. When the measurement was applied on the three devices one after another along with the NH_3 sensing time, the threshold voltage variations of these three devices were depicted in Fig.3-9. Interestingly, these three devices had similar initial threshold voltages no matter how long these devices had been exposed to the NH_3 gas. This result implied that the sensing behavior may have a strong correlation with the gate-induced carriers inside the channel.

3-2 The phenomenon of bias stress gas sensing

In section 3-1.5, we observed that bias seem to play a critical role in gas sensing. In this section we looked forward to verifying the relationship between gas sensing and bias-stress effect

3-2.1 The theory of bias stress effect

At first, we introduce the theory of bias stress effect [32]. Bias stress effect means applying a prolonged bias to the gate electrode and causes the threshold voltage shifts by creating new electronic states or defects. For a-Si TFTs two major models were developed to explain V_{th} shifts. [33.34] Although, the underlying microscopic processes are different, in both models the creation of states is governed by a dispersive process. In these models, the density of states, ΔN_D, is proportional to ΔV_{th}, since $\Delta N_D = C_{ox}\Delta V_{th}$. These states are the ones that must be filled before significant conduction can occur via accumulation layer. Thus, the more defects created during bias stress, the more holes are needed to occupy these defect states, resulting in a threshold voltage shift. In other words, the driving force for defect creation is charge trapping into defect-creation sites. Therefore, the rate at which defects are created depends on the density of free holes induced by the gate bias. In the process of gate bias stress, the free charge in the accumulation channel is replaced

by charged defects. Based on these models it is readily shown that the rate of change in V_{th} is given by differential equation [35.36]:

$$\frac{dV_{th}}{dt} \propto \frac{d(\Delta N_D}{dt} \propto N_{BT}(t)^{\alpha} \cdot \frac{t^{\beta-1}}{t_0^{\beta}} \tag{3-4}$$

where N_{BT} (t) represents the concentration of free holes in the accumulation channel. Solving equation (3-4) with α=1 yields the stretched exponential function as given:

$$V_{th} - V_{th}^{ini} = \Delta V_{th} = (V_G - V_{th}^{ini})\left\{1 - \exp\left[-\left(\frac{t}{\tau}\right)^{\beta}\right]\right\} \tag{3-5}$$

where V_{th}^{ini} is the initial threshold voltage. β is a dispersion parameter that can be extracted by plotting $\log\{-\ln[1-\Delta V_T/(V_G - V_T^{ini})]\}$ as a function of log(t) and τ represents the effective trapping time that can be expressed by

$$\tau = \frac{1}{\upsilon}\exp(\frac{E_\tau}{kT}) \tag{3-6}$$

where ν is an attempt to escape frequency that approximates 10^5 Hz.[9] and k is the Boltzamann's constant. E_τ is the mean activation energy for the defect generation

and can be obtained by measuring the stretched exponential curves at different temperatures. According to equation (3-6), in a plot of the form log (τ) as a function of 1/T, the slope of this curve represents the activation energy for defect creation, $E\tau=Ea/\beta$. In other words, the value of $E\tau$, is a measure of the device stability.

3-2.2 The phenomenon of bias stress gas sensing

In order to study the phenomenon of bias stress gas sensing in detail, we designed the following experiments:

Firstly, we measured the devices with bias stress of -7V、-11V、-15V. The results are shown in Fig.3-10. When the gate bias was increased, the threshold voltage shift was also increased. Then, we used the log scale to illustrate the experiment result as shown in Fig.3-11. It is found that the threshold voltage has a power law dependence on time. In other words, the experiment result is the same with the theory of bias stress effect.

Next we measured four identical devices with different amount of ammonia under -7V gate bias stress. We supposed that if the gate bias stress is the most important factor in the sensing mechanism, no matter how much ammonia we added, the threshold voltage shifts are all the same. In Fig.3-12, although we stressed bias in these devices, the concentration increases also enhanced the threshold voltage shift.

Maybe the gate bias stress and the ammonia concentration all play critical roles in the gas sensing behavior.

Then, in Fig.3-13, 3-14 we used amounts of ammonia concentration under different stressed biases. In Fig.3-13 and 3-14 we added 2μℓ and10μℓ ammonia, respectively. In the same ammonia environment, the threshold voltage shift increased when the bias stress was increased. Comparing Fig.3-13 with Fig.3-14, 10μℓ ammonia enhanced more threshold voltage shifts than 2μℓ under the same condition of gate bias stress.

Actually the bias stress effect also caused the threshold voltage shifts in the above experiment. But we look forward to studying the mechanism only between gas concentration and gate bias stress. Therefore, we subtracted the bias stress effect in Fig.3-10 from the experiment data of Fig.3-14 and showed the result in Fig. 3-15. In Fig. 3-15, the simulation formula comes from the equation (3-3). The fitting parameters are shown in Fig. 3-15. When the stressing bias is increased, the diffusion coefficient increased. The diffusion behavior became more obvious. At the same time, more and more ammonia molecules contributed to the threshold voltage variation.

3-2.3 The gas sensing mechanism under bias stress

From the above experiment, we proposed two kinds of gas sensing mechanism under bias stress.

3-2.3.1 Charge- trapped states

We considered the NH_3 molecules are absorbed onto the surface of active material or absorbed into the film through diffusion. The absorptive behavior between NH_3 molecules and pentacene molecules could result in charge-trapped state in pentacene film. Therefore we observed the threshold voltage shift in the environment with ammonia gas. When we increased the concentration of ammonia, the diffusion became more obvious. Much more ammonia molecules can react with pentacene and enhanced the variations of threshold voltage.

3-2.3.2 Dipole molecules

In the beginning, the ammonia is absorbed onto the surface of active material. Then the ammonia molecules diffuse into the pentacene film through the grain boundary. Because ammonia is a dipole molecule, bias stress can enhance the NH_3 molecule to absorb onto the surface of pentacene or diffused into the film. Moreover pentacene-based OTFT is a p-type transistor. We need to bias negative voltage for accumulation. In this condition, the ammonia molecules diffuse into the active layer and produce an opposite electronic field in the pentacene film. In other words, we

have to apply much more negative bias to overcome the ammonia-induced electronic field to turn-on the device. The explaination is consist with our experimental result.

Chapter 4

Conclusion

In this study we showed that the NH_3 molecules are absorbed onto the surface of active material and diffuse into the film. The absorptive behavior between NH_3 molecules and pentacene molecules result in the variation of threshold voltage. The threshold voltage shift may originate from creating charge-trapped states of pentacene and polar molecules – ammonia.

Fick's second law can successfully explain the variations of threshold voltage in the present of ammonia. When the concentrations of NH_3 increase, the diffusion coefficient increase and much more ammonia molecules contribute to the threshold voltage shift. But we also observed that three identical devices had similar initial threshold voltages no matter how long these devices had been exposed to the NH_3 gas. This result implied that the sensing behavior may have a strong correlation with the gate bias.

In addition, we varied the value of bias stress and fixed ammonia concentration. In order to reduce the threshold voltage shifts resulting from the bias stress effect, we subtracted the bias stress effect from the experimental data. Then, we observed that the bias stress increase enhanced the variation in the threshold voltage. At the same time the diffusion coefficient also increased.

Finally, we propose that gas diffusion and gate bias both play critical roles in the ammonia gas sensing by OTFTs.

Reference

[1]. M. Pope and C.E. Swenberg, Electronic Processes in Organic Crystals and polymer,Oxford University Press, New York, 1999.

[2]. D.F. Barbe and C.R. Westgate ”Surface state parameters of metal-free phthalocyanine single crystals”. J. Phys. Chem. Solids ,**31,** 2679 (1970).

[3]. M.L. Petrova and L.D. Rozenshtein ”Field effect in the organic semiconductor” Chloranil Fiz. Tverd. Tela, Soviet Phys. Solid State, **12,** 961 (1970).

[4]. M.L. Petrova and L.D. Rozenshtein:”Field effect in the organic semiconductor chloranil. Fiz. Tverd. Tela ,Soviet Phys. Solid State, **12,** 961 (1970).

[5]. F. Ebisawa, T. Kurokawa, and S. Nara,”Electrical properties of polyacetylene-polysiloxane interface”, J. Appl. Phys, **54,** 3255 (1983).

[6]. A. Tsumura, K. Koezuka, and T. Ando” Macromolecular electronic device: Field-effect transistor with a polythiophene thin film”, Appl. Phys. Lett.,**49,** 1210 (1986).

[7]. Björn Timmer, Wouter Olthuis and Albert van den Berg,” Ammonia sensors and their applications—a review”, Sensors and Actuators B, **107,** 666 (2005)

[8]. M. Wallin, C-J. Karlsson, M. Skoglundh,” Selective catalytic reduction of NO*x* with NH_3 over zeolite H-ZSM-5: influence of transient ammonia supply”, J. Catal.,**218,** 354

[9]. X. Xuan, C. Yue, S. Li,” Selective catalytic reduction of NO by ammonia with fly ash catalyst”, Fuel **82**, 575 (2003).

[10].Steven G. Buckley, Christopher J. Damm, Wolfgang M. Vitovec,” Ammonia Detection and Monitoring with Photofragmentation Fluorescence”, Applied Optics, **37,** 8382 (1998)

[11]. L.R. Narasimhan, W. Goodman, C. Kumar," Correlation of breath ammonia with blood urea nitrogen and creatine during hemodialysis", PNAS, **98**, 4617 (2001)

[12]. D.J. Kearney, T. Hubbard, D. Putnam," Breath ammonia measurement in *Helicobacter pylori* infection", Digest. Dis. Sci, **47**, 2523 (2002)

[13]. N.K. Jain, V. Mangal, "*Helicobactor pyroli* infection in children", J. Nep. Med. Assoc, **38,** 140 (1999)

[14]. K. Zakrzewska, "Mixed oxides as gas sensors", Thin Solid Films, **391**, 229 (2001)

[15]. N. Yamazoe, "Chemical Sensor Technology", Elsevier, Amsterdam, 1991.

[16]. X. Wang, N. Miura, N. Yamazoe, "Study of WO3-based sensing material for NH_3 and NO detection", Sens. Actuators B ,**66,** 74 (2000).

[17]. C.N. Xu, N. Miura, Y. Ishida, "Selective detection of NH_3 over NO in combustion exhausts by using Au and MoO_3 doubly promoted WO_3 element", Sens. Actuators B, **65**163 (2000)

[18]. V.V. Chabukswar, S. Pethkar, A.A. Athawale", Acrylic acid doped polyaniline as an ammonia sensor", Sens. Actuators B , **77** 657 (2001)

[19]. L. Torsi, A. Dodabalapur, L. Sabbatini, P.G. Zambonin, "Multi-parameter gas sensors based on organic thin-film-transistors" Sensors and Actuators B, **67**, 312, (2000).

[20]. F. Liao, C. Chen, V. Subramanian, "Organic TFTs as gas sensors for electronic nose applications," Sensors and Actuators B, **17**, 849 (2005).

[21]. M.C. Tanese, D. Fine, A. Dodabalapur, L. Torsi, "Interface and gate bias dependence responses of sensing organic thin-film transistors," Biosensors and Bioelectronics, **21**, 782 (2005).

[22]. B. Crone, A. Dodabalapur, A. Gelperin, L. Torsi, H. E. Katz, A. J. Lovinger, and Z. Bao "Electronic sensing of vapors with organic transistors," Appl. Phys. Lett., **78**, 3965, (2001).

[23]. L. Torsi, M.C. Tanese, N. Cioffia, M.C. Gallazzi,L. Sabbatini, and P.G. Zambonin, "Alkoxysubstituted polyterthiophene thin-film-transistors as alcohol sensors," Sensors and Actuators B, 98, 204,(2004)

[24]. B. Crone, A. Dodabalapur, A. Gelperin," Electronic sensing of vapors with organic transistors" Appl Phys Lett **78**, 2229, (2001)

[25] JB Chang,"Functionalized Polythiophene Thin-film Transistors for Low-cost Gas Sensor Arrays",eecs.berkeley.edu, 2006

[26]. Torsi L, Lovinger AJ, Crone B, "Correlation between Oligothiophene Thin Film Transistor Mophology and Vapor Response", J Phys Chem B, **106**, 12563 (2002)

[27]. Liang Wang, Daniel Fine, and Ananth Dodabalapur," Nanoscale chemical sensor based on organic thin-film transistors", Appl. Phys. Lett., **85**, 6386, 2004.

[28]. C. D. Dimitrakopoulos, A. R. Brown, and A. Pomp, "Molecular beam deposited thin films of pentacene for organic field effect transistor applications", J. Appl. Phys.,**80**, 2501, (1996)

[29]. Chih-Wei Chu, Sheng-Han Li, Chieh-Wei Chen,"High-performance organic thin-film transistors with metal oxide/metal bilayer electrode", Appl. Phys. Lett., **87**, 193508, (2005).

[30]. A.Alec Talin, Luke L. Hunter, François Léonard," Large area, dense silicon nanowire array chemical sensors" , Appl. Phys. Lett. **89**, 153102 (2006)

[31].Oana D. Jurchescu, Jacob Baas, and Thomas T. M. Palstra," Electronic transport properties of pentacene single crystals upon exposure to air", Appl. Phys. Lett. **87**, 052102 ,(2005)

[32].Henrique L. Gomes, Peter Stallinga, Franco Dinelli, “Electrical characterization of organic based transistors: stability issues”,Polym.Adv. Technol.**16**, 227,(2005).

[33]. Jackson WB, Marshall JM,” Role of hydrogen in the formation of metastable defects in hydrogenated amorphous silicon**”** Phys. Rev. B ,39,1164 (1989)

[34]. Crandall RS.” Defect relaxation in amorphous silicon: Stretched exponentials, the Meyer-Neldel rule, and the Staebler-Wronski effect**”** Phys Rev. B, **43**,4057 (1991)

[35]. Wehrspohn RB, Deane SC, French ID, “Relative importance of the Si–Si bond and Si–H bond for the stability of amorphous silicon thin film transistors.” J. Appl. Phys.,**87**, 144 (1999).

[36]. Wehrspohn RB, Deane SC, French ID, “Effect of amorphous silicon material properties on the stability of thin film transistors: evidence for a local defect creation model ‘J. Non-Cryst. Solids, **266**, 459(2000)

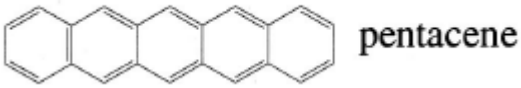

Fig. 1-1 Molecular structure of pentacene.

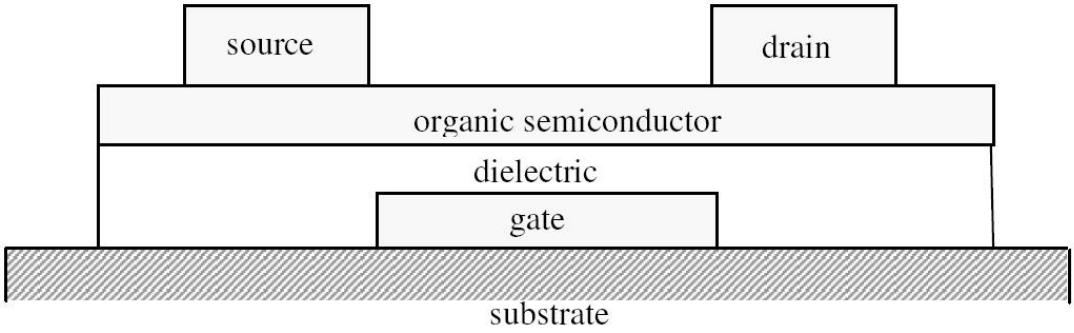

Fig. 1-2 (a) Top contact structure.

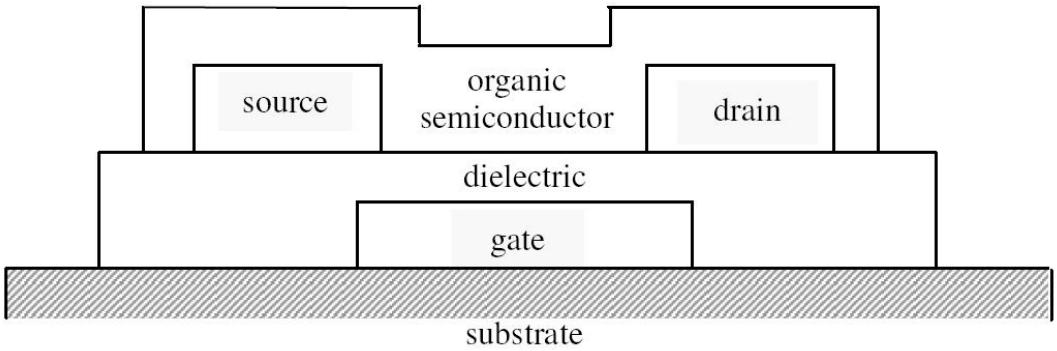

Fig. 1-2 (b) Bottom contact structure.

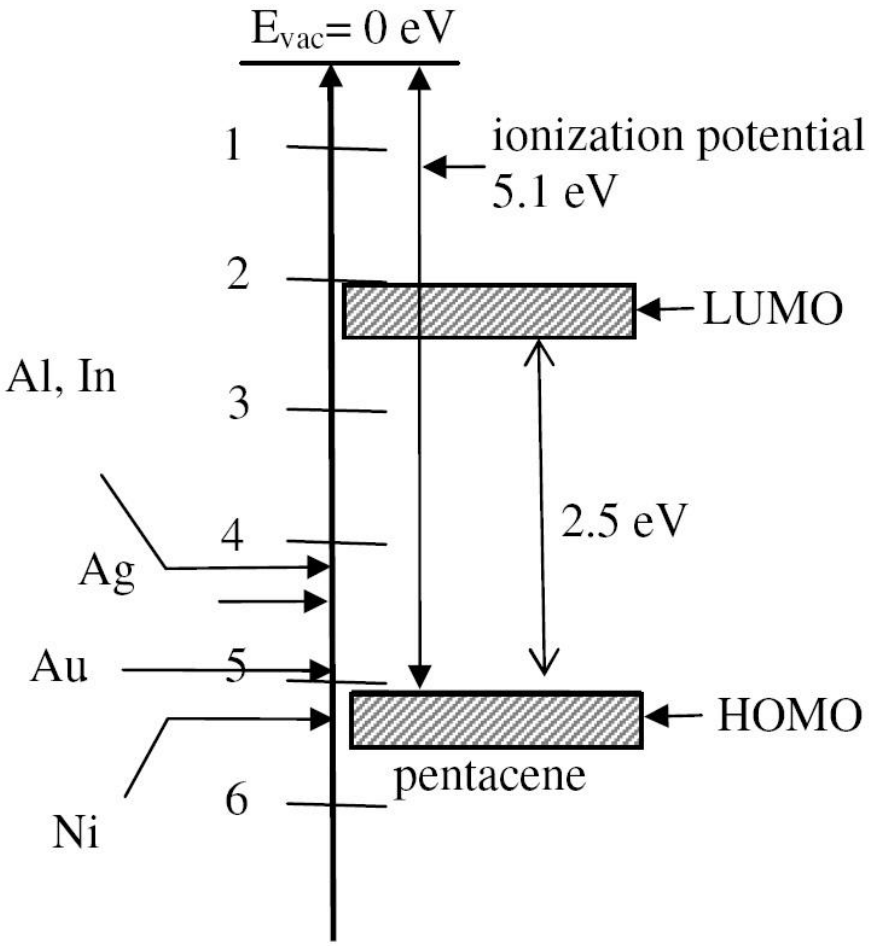

Fig. 1-3 The work function of various metals and ionization potential of pentacene.

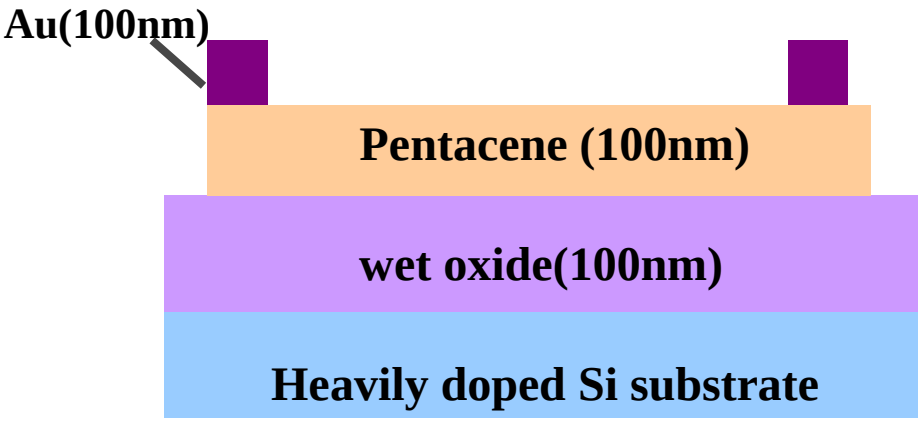

Cross

Fig. 2-1 Conventional bottom-gate top-contact OTFTs were used in this experiment.

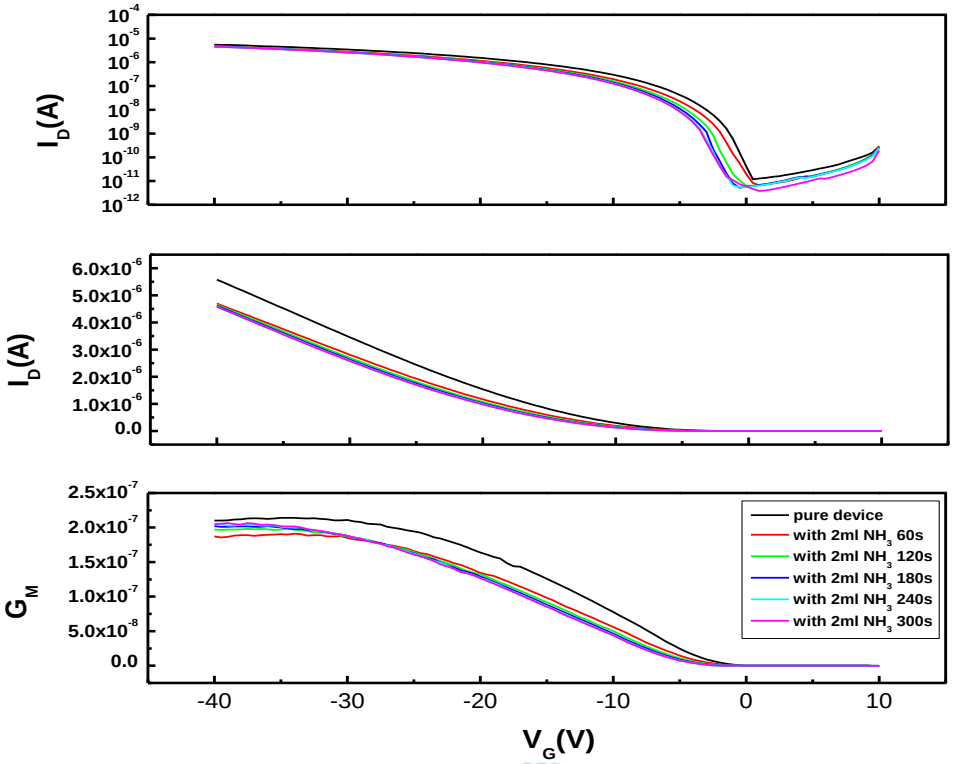

Fig. 3-1 The electrical properties of OTFT adding 2μℓ NH_3.

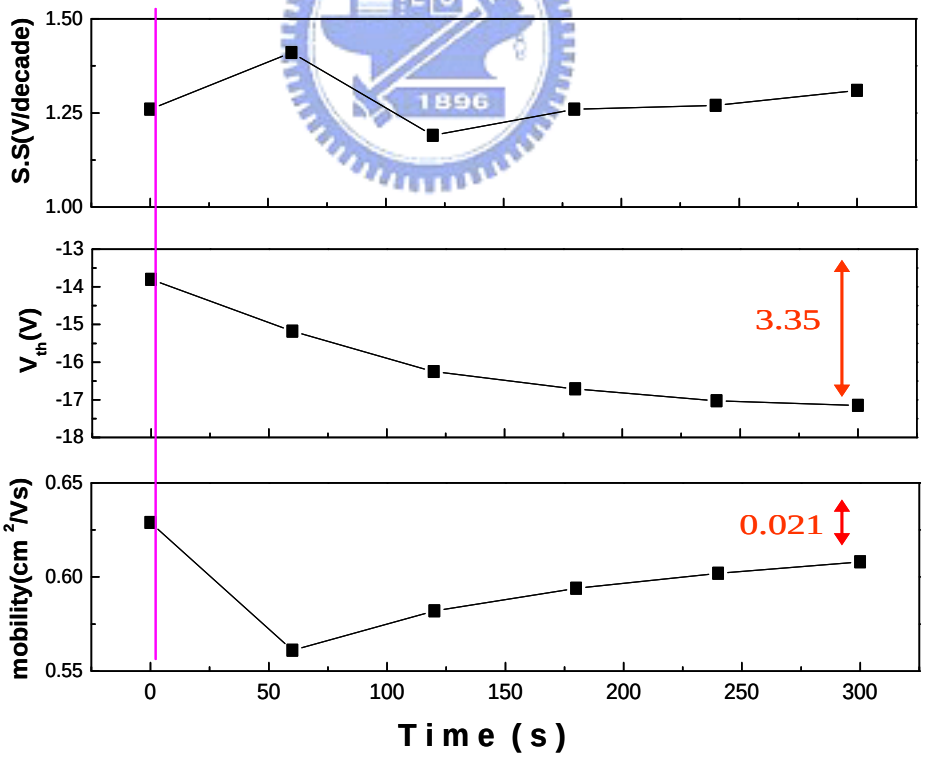

Fig. 3-2 The variations of subthreshold swing、threshold voltage and mobility along with time in environment of 2μℓ NH_3 (after pink line).

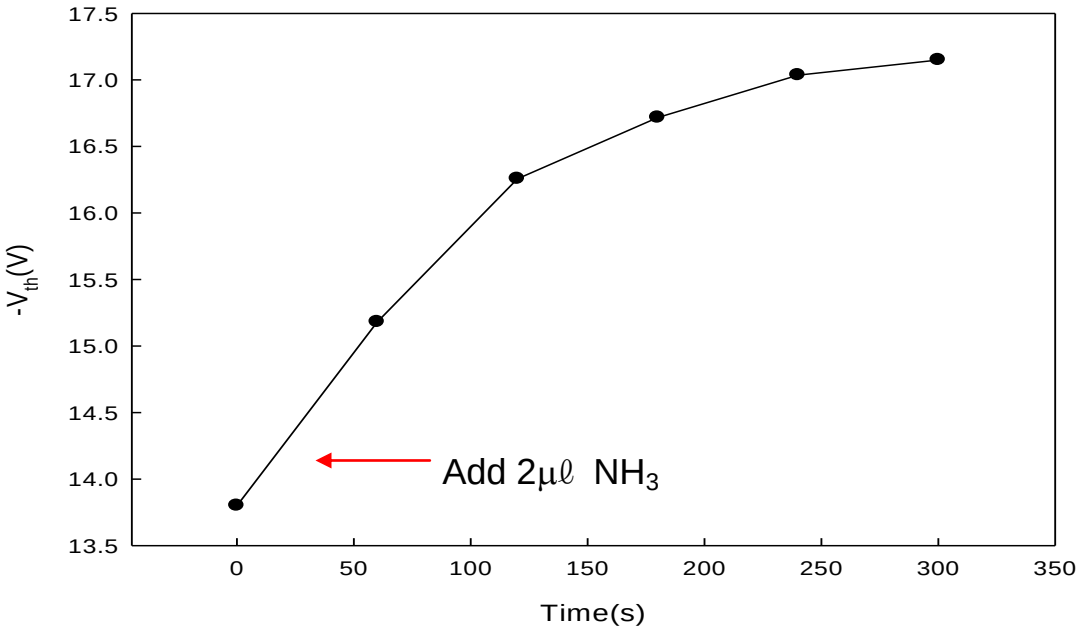

Fig. 3-3 The variations of threshold voltage along with time in environment of 2μℓ NH_3

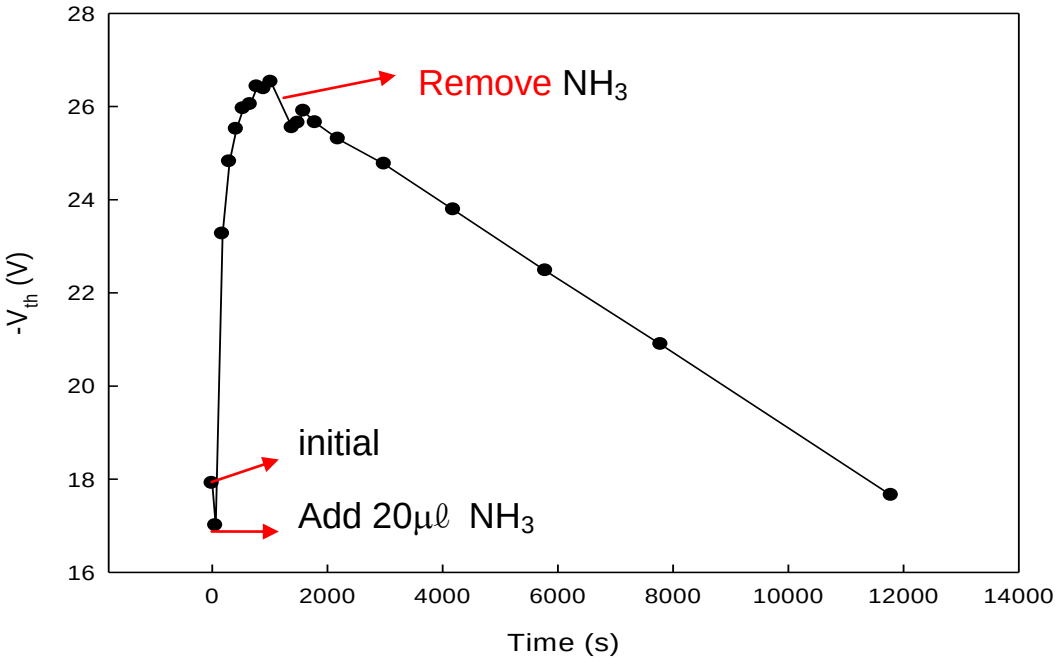

Fig. 3-4 When NH_3 was removed, the threshold voltage tended to recover.

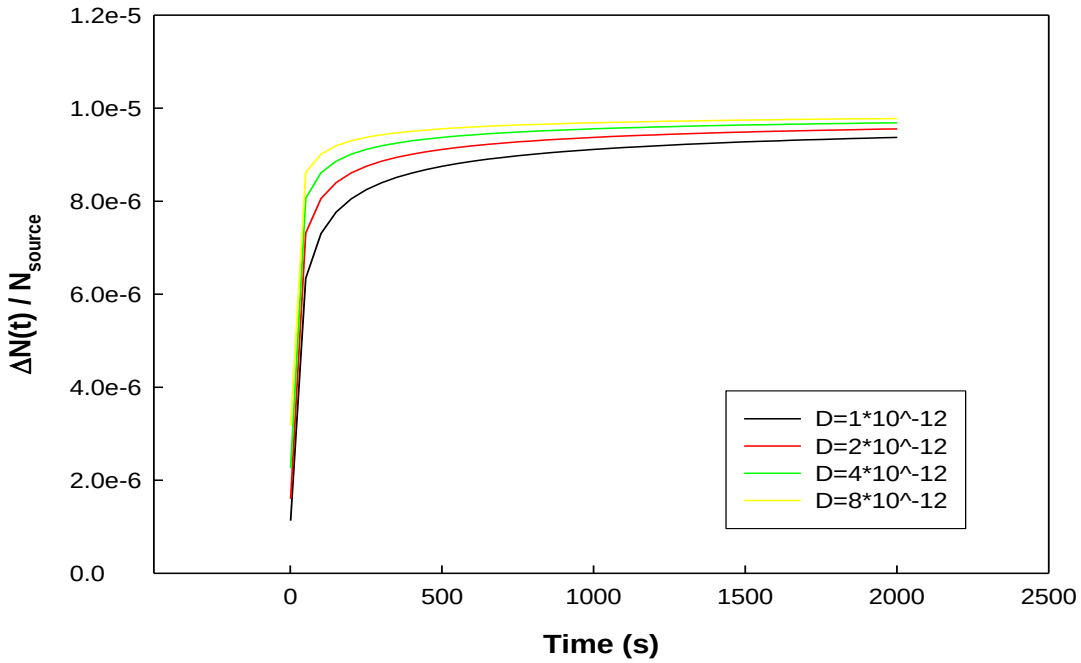

Fig. 3-5 The fitting curve of Fick's second law are in the condition of d=10^{-5} cm and D=10^{-12} cm^2/s、2*10^{-12} cm^2/s、4*10^{-12} cm^2/s、8*10^{-12} cm^2/s

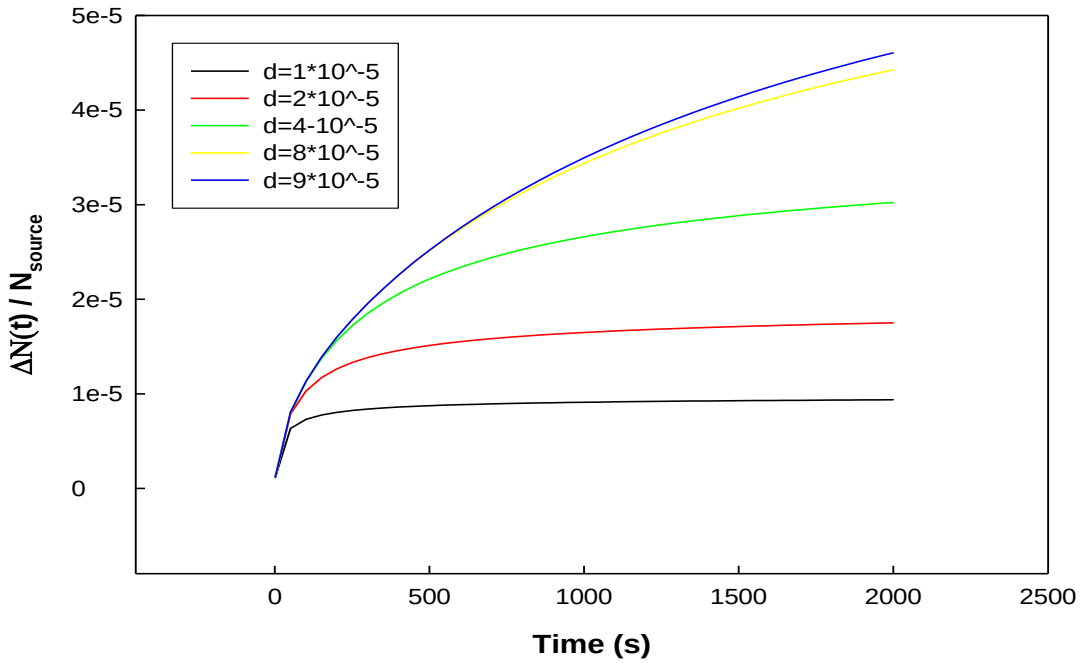

Fig. 3-6 The fitting curve of Fick's second law are in the condition of D=10^{-12} cm^2/s and d=10^{-5} cm、2* 10^{-5} cm、4*10^{-5} cm、8*10^{-5} cm、9*10^{-5} cm.

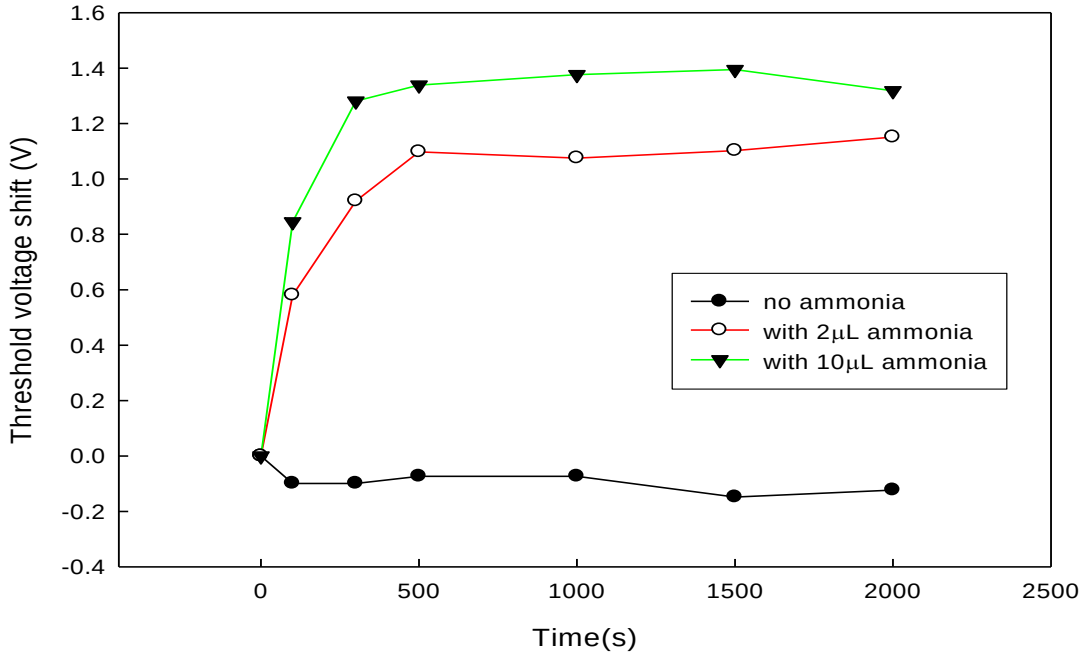

Fig. 3-7 The threshold voltage shift in different amount of NH_3.

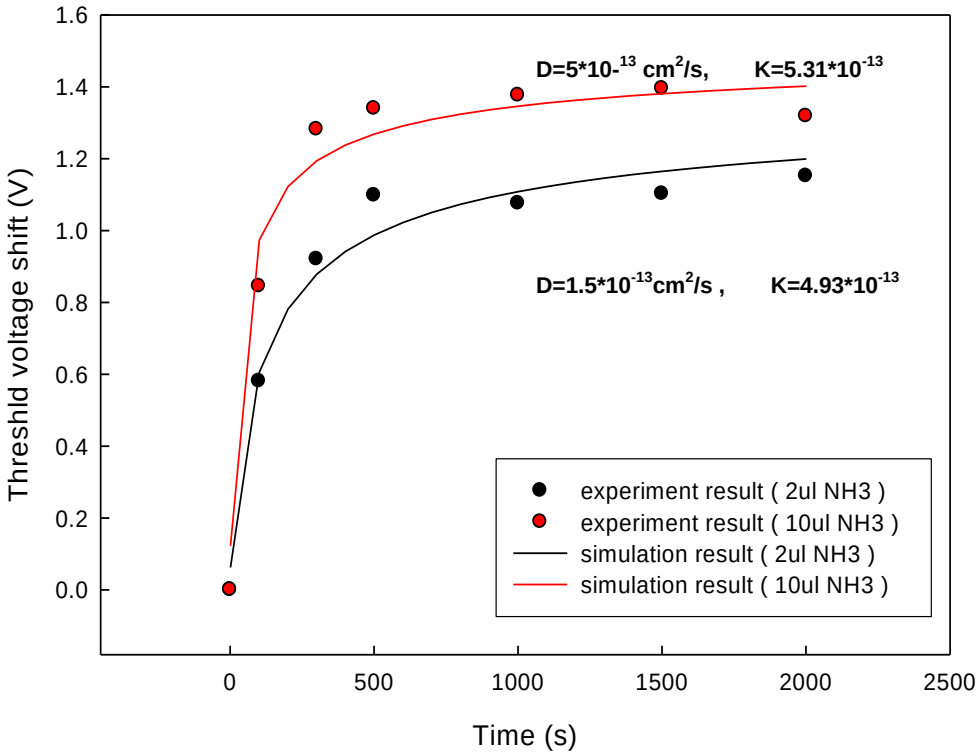

Fig. 3-8 The dependence of threshold voltage shift on sensing time in the environments with different NH_3 concentrations. The circles are experiment data. The curves are the fitting result from Fick's second law.

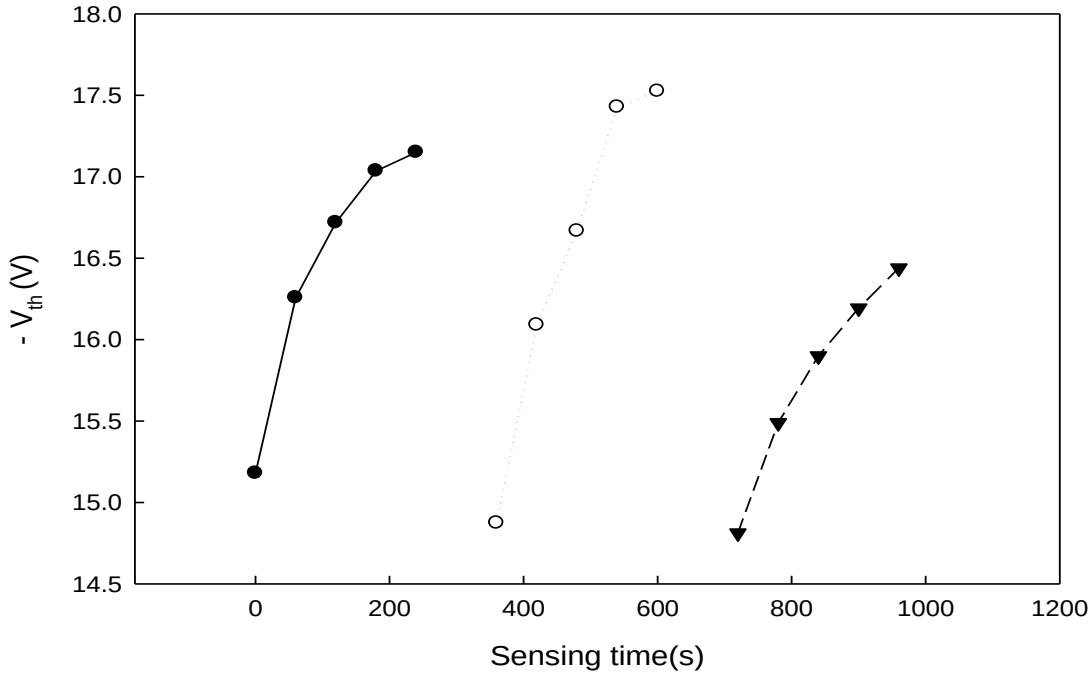

Fig. 3-9 The threshold voltage variation of three identical devices measured one after another in the environment with NH_3 gas. The NH_3 amount injected into the cotton mass was 2μℓ.

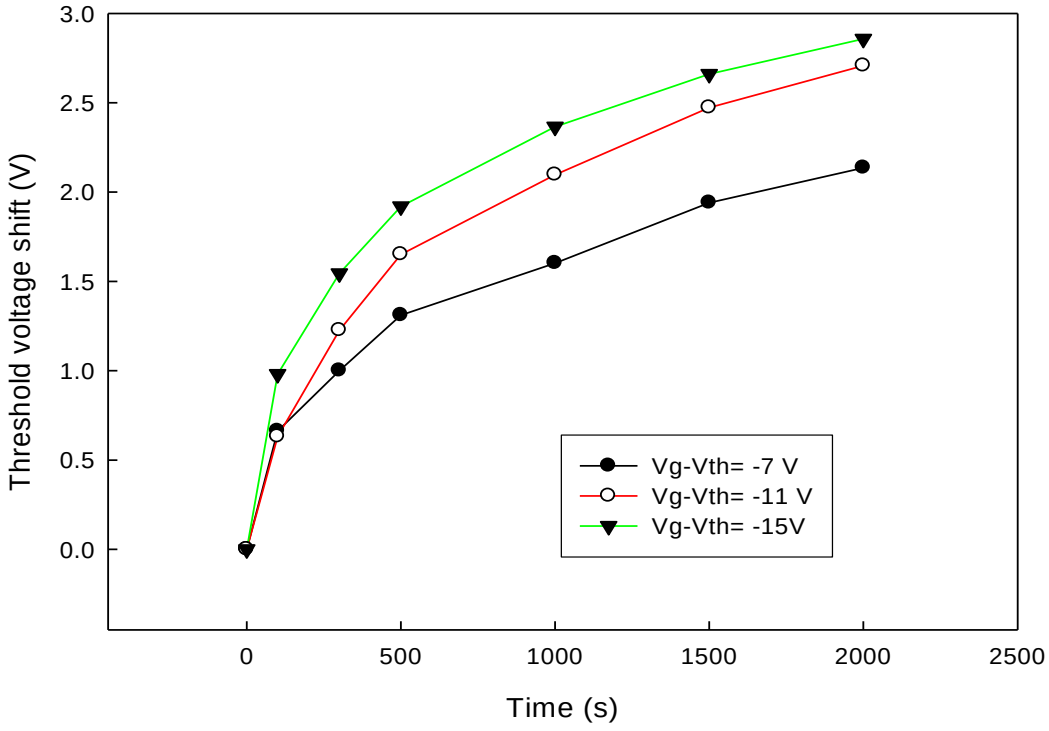

Fig. 3-10 The threshold voltage shift in different bias stress conditions

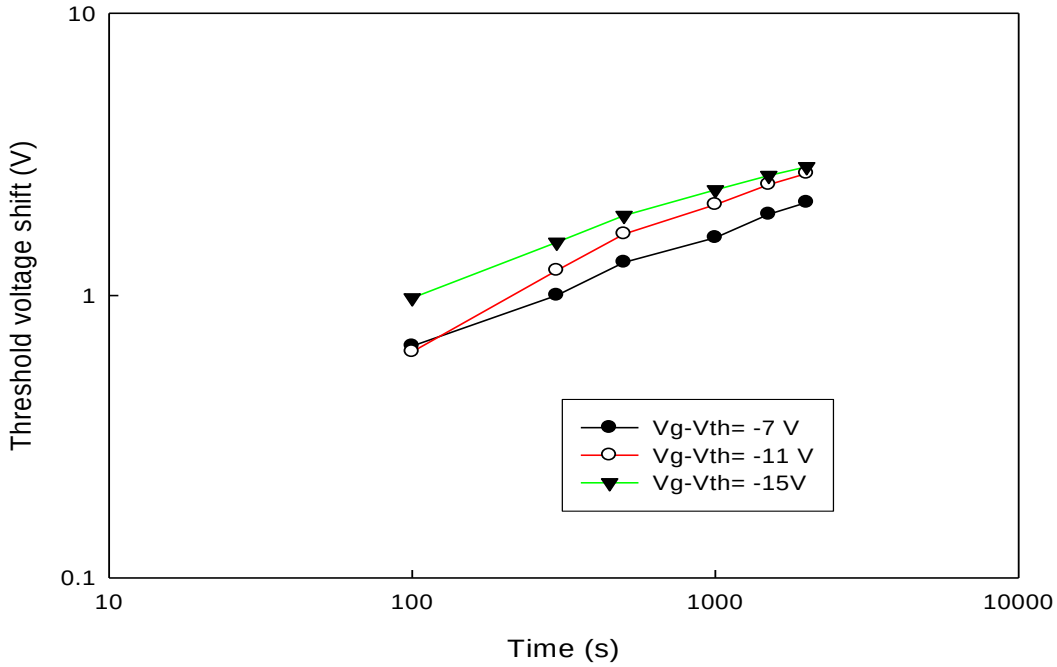

Fig. 3-11 The threshold voltage shift in different bias stress conditions

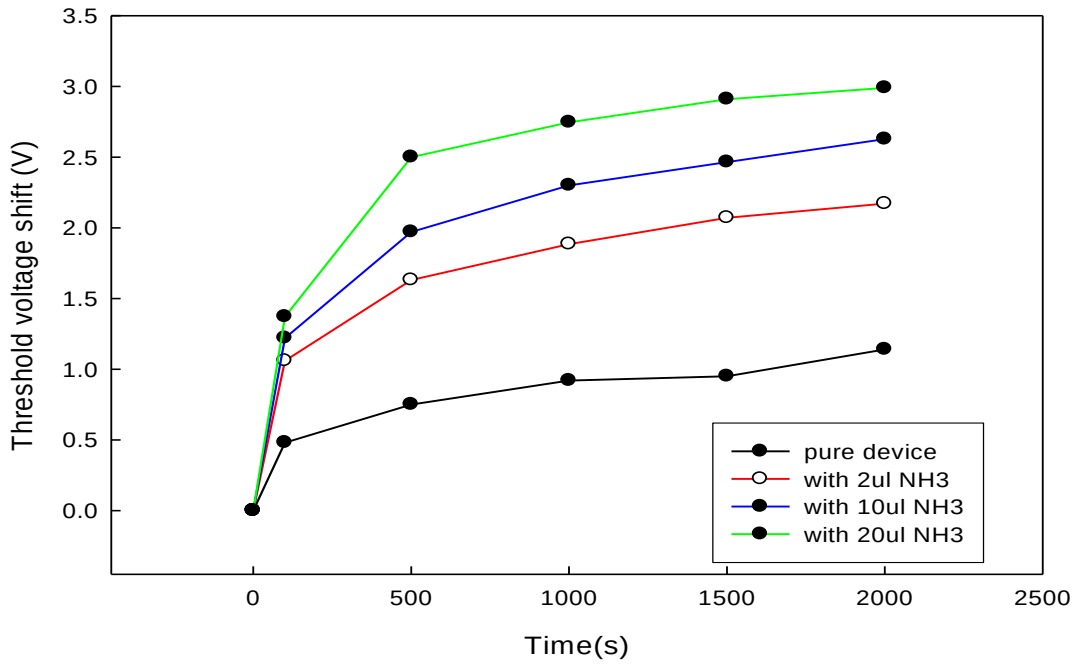

Fig. 3-12 The threshold voltage shift in different amount of concentrations with V_g-V_{th}^{ini}= -7V bias stress.

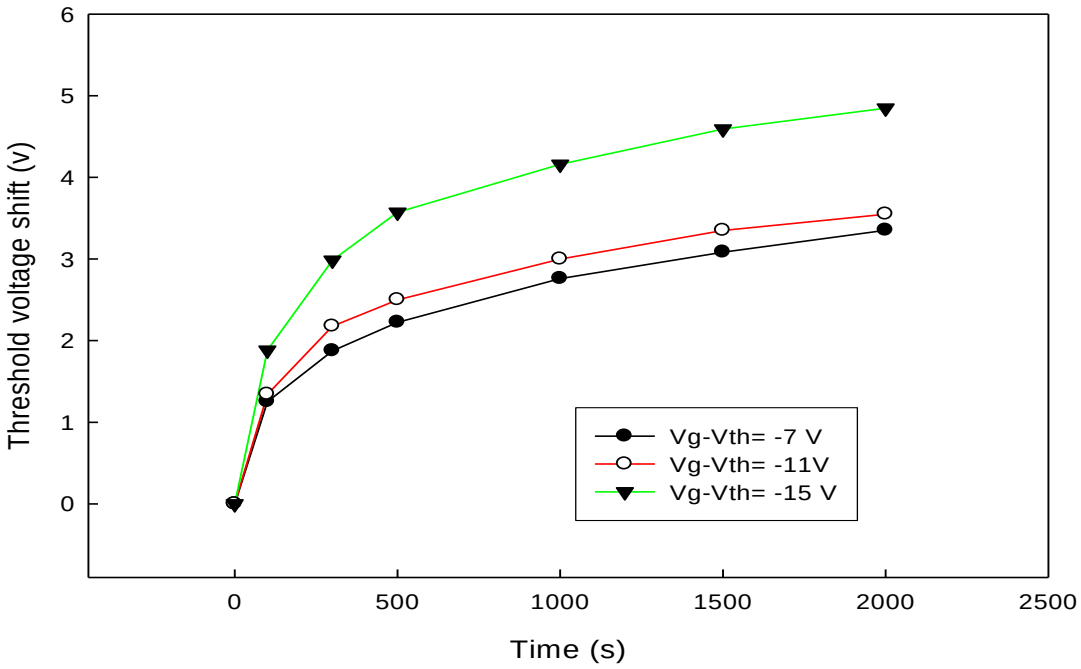

Fig. 3-13 The threshold voltage shift in the environment of 2μℓ ammonia with different amount of bias stress.

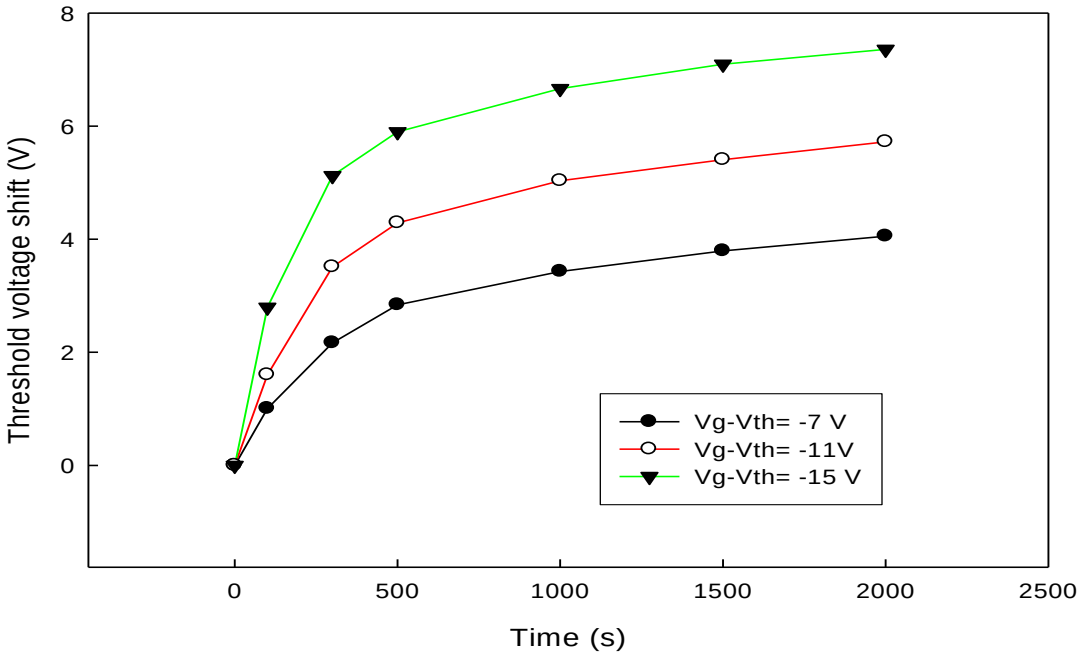

Fig. 3-14 The threshold voltage shift in the environment of 10μℓ ammonia with different amount of bias stress.

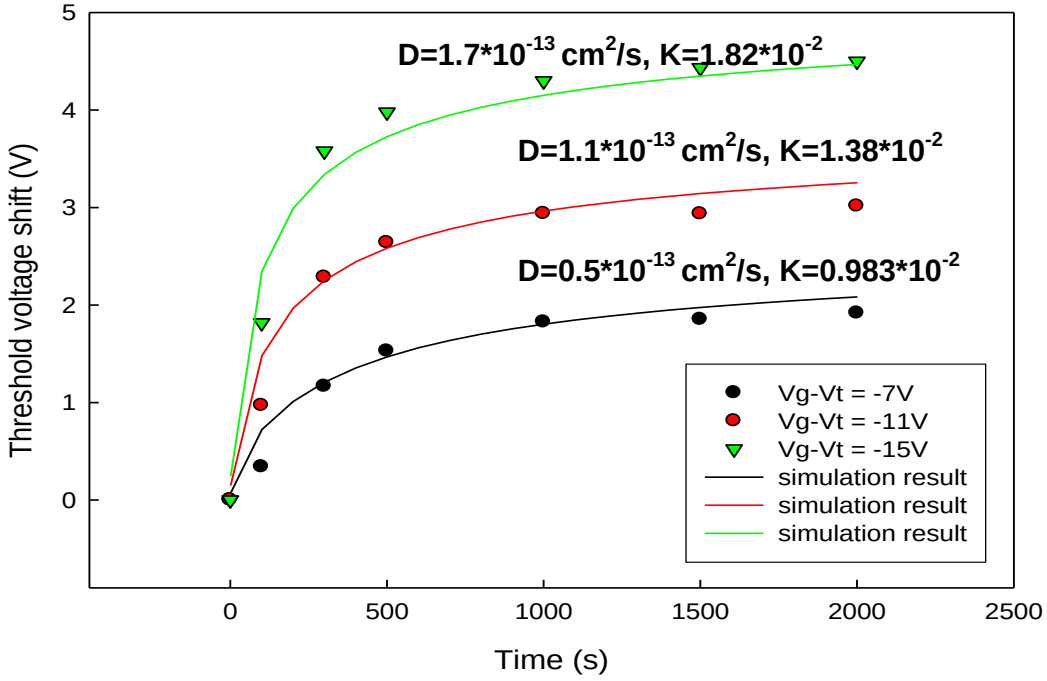

Fig. 3-15 The dependence of threshold voltage shift on sensing time in the environments with different gate bias strees. The circles are experiment data. The curves are the fitting result from Fick's second law.